RASĀYAN *J. Chem.*
Vol. 19 | No. 2 | 914-920| April-June | 2026
ISSN: 0974-1496 | e-ISSN: 0976-0083 | CODEN: RJCABP
http://www.rasayanjournal.com
http://www.rasayanjournal.co.in

GREEN SYNTHESIS OF IRON AND COPPER DOPED Ag/AgCl NANOPARTICLES USING *Ocimum kilimandscharicum* LEAF EXTRACT

T.Geetha[1,✉], J. K. Smitha [2], L. M. Irimpan[3], M. Sebastian[4], C. J. Theresa[4], B. Joseph[4], M. Nancy[1], K. Nimmy[1], and K. C. Dhanya[5]

[1]Department of Chemistry, Vimala College(Autonomous), Thrissur-680009, (Kerala) India
[2]Department of Soil Science and Agricultural Chemistry, Kerala Agriculture University, Thrissur-680656, (Kerala), India
[3]Department of Physics, Vimala College(Autonomous), Thrissur-680009, (Kerala) India
[4]Department of Chemistry, St. Mary's College(Autonomous), Thrissur-680020, (Kerala) India
[5]Department of Microbiology, St. Mary's College(Autonomous), Thrissur-680020, (Kerala) India
✉Corresponding author: geethamukundant@gmail.com

ABSTRACT

Nanoparticles of Ag/AgCl, AgCl doped with iron oxide and Ag/AgCl doped with copper oxide were synthesised from silver nitrate solution using *Ocimum kilimandscharicum* leaf extract without any additional source of chloride ions. Formation of nanoparticles was validated by X-ray Powder Diffraction data, Fourier Transform Infrared Spectra and data obtained from Scanning Electron Microscopy coupled with Energy Dispersive X-ray Spectroscopy. Doping was observed to affect both the morphological features of the prepared nanoparticles and their antibacterial activity. Copper-doped Ag/AgCl nanoparticles were irregularly shaped with rounded edges, while doping with iron resulted in the formation of cube-shaped AgCl nanoparticles. Ag/AgCl nanoparticles, Cu doped Ag/AgCl nanoparticles, and Fe-doped AgCl nanoparticles were all effective against bacterial strains of *Pseudomonas*, *Bacillus* and *Staphylococcus* sp., though Cu doped Ag/AgCl nanoparticles was more effective than the rest. This study highlights the significant role of doping in enhancing antibacterial efficacy and in modulating the morphological characteristics of nanoparticles.

Keywords: Silver Nanoparticles, Silver Chloride Nanoparticles, Doping, Antibacterial Activity, Environmentally Friendly Synthesis.

RASĀYAN *J. Chem.*, Vol. 19, No.2, 2026

INTRODUCTION

In an era when nanomaterials, especially metal nanoparticles, are emerging as a solution to some of the most pressing problems of society, especially in the area of health and environment, what if these could be synthesised using plant phytochemicals, and their properties, like morphology and antibacterial activity, could be fine-tuned by doping? In this study, we attempt to synthesise nanoparticles of silver and its salt (like silver chloride) using plant phytochemicals and to modify and fine-tune its properties by doping. Nanoparticles (NPs) of silver, and their salts (like silver chloride), have been used as an antimicrobial agent in both medical and non-medical areas. The unique physicochemical properties, like high surface-to-volume ratios, enhanced reactivity, and tunable optical properties of the NPs, make them suitable for application in the areas of drug therapies, drug delivery, antimicrobial coatings, sensors, and catalysis. Ag/AgCl-NPs, on light exposure, have the ability to produce reactive oxygen species that can damage the cell membrane and thus destroy the ability of bacterial cells to protect themselves. Their ability to release silver ions into the environment in a sustained manner is responsible for its enhanced antibacterial activity[1]. The traditional chemical methods of synthesising NPs employ hazardous chemicals and are often energy-intensive. Moreover, these chemicals may remain on the surface of synthesised silver nanoparticles as residues and thus can pose a significant risk, particularly when these NPs are used in drug delivery, antimicrobial treatments, cosmetics, or other applications where they come in contact with the human body. The search for nontoxic and green, synthetic technologies has led to the use of biological

http://doi.org/10.31788/RJC.2026.1929607

systems and plant extracts in NP synthesis. This method utilises plant extracts as reducing and capping agents and is favoured because they are biocompatible, eco-friendly, nontoxic, and cost-effective compared to traditional chemical methods.[2] Recent research has focused on antimicrobial properties of novel bimetallic nanoparticles, doped nanoparticles, or nano alloys and differences in their antibacterial properties.[3] In this study, we attempt to synthesise Ag/AgCl nanoparticles, Ag/AgCl nanoparticles doped with iron oxide and Ag/AgCl nanoparticles doped with copper oxide and to compare their antibacterial properties. This aligns with Sustainable Development Goals 12, as the use of plant extracts eliminates the use of harmful chemicals in nanoparticle synthesis and minimises the production of toxic waste.[4]

EXPERIMENTAL

Materials

Analytical grade reagents of ferric nitrate ($Fe(NO_3)_3.9H_2O$), copper nitrate ($Cu(NO_3)_2.3H_2O$) and silver nitrate ($AgNO_3$) were purchased from Merck, India, and used directly without additional purification. Fresh leaves of *Ocimum kilimandscharicum* (Karpoora Tulasi/camphor basil) were collected locally from Thrissur, Kerala, India.

Synthesis of Nanoparticles

Fresh leaves of Ocimum kilimandscharicum (Karpoora Tulasi/camphor basil) were washed repeatedly with double-distilled water to eliminate adhering dirt and dust. The collected leaves were first dried, ground to a fine powder, and stored in a plastic airtight container at room temperature. The leaf extract was prepared by adding 5 g of dried leaf powder to 500 mL of distilled water and boiling the mixture for 15 minutes. The mixture was then filtered (Whatman number 41), and the filtrate was stored in the refrigerator for further experimentation. To synthesise Ag/AgCl nanoparticles (NPs), 50 mL of $AgNO_3$ solution (0.1M) was added to 50 mL of plant extract while stirring continuously on a magnetic stirrer. The stirring continued for 30 minutes, after which the solution was stored in a cool, dark chamber overnight. The solution was centrifuged the next day to separate nanoparticles. To synthesise iron/iron oxide and copper/copper oxide NPs, 0.1M $Fe(NO_3)_3.9H_2O$ and $Cu(NO_3)_2.3H_2O$ were used as the precursors. Ag/AgCl nanoparticles doped with iron oxide were prepared by adding 120 mL of 0.1M ferric nitrate to 200 mL of plant extract, followed by 80 mL of 0.1M silver nitrate solution. Metal salt solution was added in a dropwise manner with continuous stirring, and the stirring continued for half an hour after the addition was completed. The solution was stored overnight in a cool, dark chamber and centrifuged the next day to separate nanoparticles. Ag/AgCl nanoparticles doped with copper oxide were prepared in a similar manner using a 0.1M copper nitrate $Cu(NO_3)_2.3H_2O$ solution. The synthesised nanoparticles were dried and subsequently stored in a sealed vial for further experimental analysis.

Characterisation of Nanoparticles

The synthesised nanoparticles were characterised by X-ray Powder Diffraction (XRD), Fourier Transform Infrared Spectroscopy (FTIR) and Scanning Electron Microscopy with Energy Dispersive X-ray Spectroscopy (SEM-EDX). Powder XRD patterns of the samples were recorded using a PANalytical XRD system in the Bragg angle range of 5° to 90°. Infrared spectra were recorded using a Cary 620 FTIR Imaging system combined with a Cary 660 FTIR Spectrometer. The FTIR spectra of nanoparticles were recorded in transmission mode by scanning the sample in the range between 400 and 4000 cm^{-1}. The information about the chemical composition of a sample was obtained from SEM–EDX.

Antibacterial Assay

Antibacterial tests were carried out by the Kirby-Bauer method (KB test) or the well diffusion method with some modifications. *E coli, Pseudomonas sp*, *Bacillus sp*, and *Staphylococcus sp*. cultures were inoculated into a 250 mL conical flask containing 100 mL of nutrient broth. From this, 0.1 mL of culture was uniformly distributed into nutrient agar plates. Wells of 4 mm diameter were punched aseptically with a sterile tip. Samples were dissolved in dimethyl sulfoxide. A volume of 20 µl of samples at different concentrations was introduced into the well. The plates were then incubated at 37 ^{0}C for 16-18 hours and examined for the presence of a zone of inhibition.[5]

RESULTS AND DISCUSSION

On adding a freshly prepared solution of silver nitrate to the aqueous extract of *Ocimum kilimandscharicum*, ~~the~~ colour of the solution turned reddish brown. The observed colour change suggests that the metal ions in the precursor, viz. Ag^{+} may have been reduced to zero valent metal (Ag^{0}) by the various biomolecules present in the leaf extract.[6] *Ocimum kilimandscharicum* is rich in secondary metabolites like methyl eugenol, camphor, γ-cadinene, borneol, linalool, and limonene. In addition to acting as reducing agents, these biomolecules are also capable of stabilising the nanoparticles.[7,8] Studies have previously reported the formation of silver chloride (AgCl) and silver-silver chloride nanoparticles (Ag/AgCl) NPs from silver nitrate solution using plant extract without any other external source of chloride ions. The occurrence of chloride ions in plant extracts has been previously reported, and it is these chloride ions that may act as a source of chlorine for the formation of Ag/AgCl nanoparticles.[9–12] On adding a freshly prepared solution of ferric nitrate to the aqueous extract of *Ocimum kilimandscharicum*, the colour of the solution turned brownish black, while it turned yellowish red on adding copper nitrate. The observed colour change suggests that the metal ions in the precursor may have been converted to oxide or hydroxides, or they may have formed complexes with the various phytochemicals present in the leaf extract. During the synthesis of iron-doped Ag/AgCl NPs, the colour of the solution changed to brownish black, while the colour changed to yellowish brown for copper-doped Ag/AgCl NPs. The colour change suggests the successful formation of doped Ag/AgCl NPs. By eliminating the use of hazardous reducing agents such as sodium borohydride and hydrazine, as well as synthetic capping agents like polyvinylpyrrolidone (PVP), the present green synthesis approach adheres to the principles of Sustainable Development Goal 12, promoting responsible consumption and environmentally sound production practices.

X-Ray Diffraction Analysis

The XRD patterns of the as-synthesised copper and iron NPs is shown in Fig.-1(a), and that of Ag/AgCl NPs and Cu and Fe doped AgCl NPs is given in Fig.-1(b). The XRD patterns of the as-synthesised iron and copper NPs lacks well-defined peaks. The broadness of the observed peak suggests that the synthesised nanoparticles were amorphous in nature or of very small crystallite size.[13]

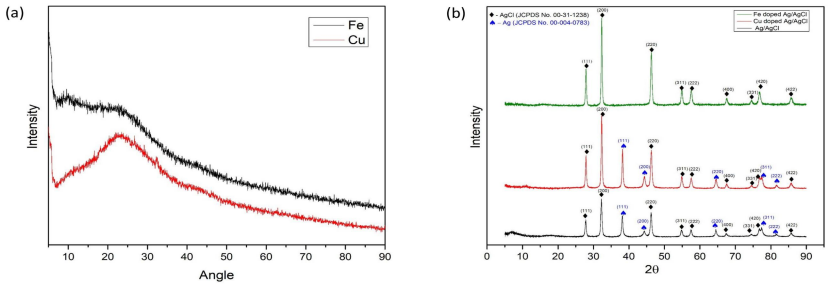

Fig.-1: XRD Patterns of (a) the as-synthesised Cu and Fe NPs (b) as-synthesised Ag/AgCl NPs and Cu and Fe doped AgCl NPs

In Fig.-1(b), the sharp, well-defined peaks in the XRD pattern reveal the distinctive crystalline characteristics of the synthesised NPs. As can be seen from the image, the Ag/AgCl NPs show diffraction peaks at 2θ values of 27.78, 32.22, 38.11, 44.24, 46.22, 54.75, 57.41, 64.49, 67.38, 74.43, 76.71, 77.39, 81.47 and 85.61º. The peak at 27.78, 32.22, 46.22, 54.75, 57.41, 67.38, 74.43, 76.71 and 85.61º can be assigned to AgCl (Reference no. 00-031-1238) with the corresponding Braggs planes being (111), (200), (220), (311), (222), (400), (331), (s420) and (422) of cubic AgCl. The peaks at 38.11, 44.24, 64.49, 76.71, 77.39 and 81.47º can be assigned to Ag (Reference no. 00-004-0783) with the corresponding Bragg's planes being (111), (200), (220), (311) and (222) of cubic Ag Nanoparticles. This confirms the successful biosynthesis of silver and silver chloride nanoparticles (Ag and AgCl NPs). The average crystallite size was determined from the X-ray diffraction peak broadening using the Debye-Scherrer formula:

$$D = \frac{0.9\lambda}{\beta \cos\theta}$$

Where D is the average crystallite size in nanometers, λ is the X-ray wavelength of Copper, β is the full width at half maximum of the peak in radians, and θ is the Bragg's angle. Using Scherer's equation, the average crystallite sizes of AgCl NPs were estimated to be 47 nm, and that of Ag NP to be 26 nm, respectively. The diffraction pattern of the synthesised copper-doped NPs was very similar to the Ag/AgCl NPs with peaks at 27.89, 32.28, 32.34, 38.15, 44.42, 46.41, 54.85, 57.58, 64.54, 67.52, 74.49, 76.77, 77.55, 81.51 and 85.65º. Of these, peaks at 27.89, 32.28, 38.15, 46.41, 54.85, 57.58, 67.52, 74.49, 76.77 and 85.65º can be assigned to cubic AgCl (Reference no. 00-031-1238), and those at 38.15, 44.42, 64.54, 77.55, and 81.51º can be assigned to cubic Ag (Reference no. 00-004-0783). The peak at 32.34 may originate from AgO formed by surface oxidation of silver nanoparticles. The calculated crystallite sizes of AgCl and Ag NPs were 47 and 54 nm, respectively. On the other hand, the diffraction pattern of iron-doped NPs showed peaks at 27.87, 32.29, 46.27, 54.87, 57.51, 67.48, 74.46, 76.76 and 85.62 º. It is interesting to note that all of the peaks in the diffraction pattern can be assigned to cubic AgCl (Reference no. 00-031-1238), and the peaks attributed to silver nanoparticles are missing.

FTIR

The Ag/AgCl NPs, Cu doped Ag/AgCl NPs, and Fe-doped Ag/AgCl NPs were analysed by FTIR. The resultant spectra are shown in Fig.-2 and the peaks are listed in Table-1. The pattern of bands in the spectra is remarkably similar, indicating similarity in biomolecules that act as capping agents in nanoparticle synthesis.

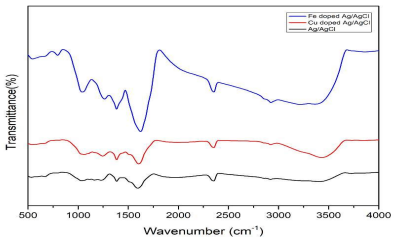

Fig.-2: FTIR Spectra of the as-synthesised Ag/AgCl NPs and Cu and Fe Doped AgCl NPs

Table-1: FTIR Functional Group Analysis

S. No.	Ag/AgCl NP	Fe-doped AgCl NPs	Cu-doped Ag/AgCl NPs	Functional group
1.	3409.55	3363.27	3432.69	O-H stretching of polyphenols, alcohol/ N-H stretching of amine
2.	2923.57	2923.57	2923.57	C-H stretching of the methyl or methylene group
3.	2352.74	2352.74	2352.74	C=O of CO_2
4.	1596.78	1619.92	1604.49	C=C stretching of alkenes or aromatics/C=O
5.	1388.50	1380.79	1388.50	C-H bending/Phenolic OH
6.	1234.22	1265.08	1241.94	C-O-C stretching of ethers
7.	1033.66	1041.37	1064.52	C-O stretching of alcohol/ethers
8.	532.00	547.68	532.20	Ag-Cl stretching

A broad band between 3450-3250 cm^{-1} was seen in all FTIR spectra, indicating the occurrence of either a hydroxyl group, an amine group or adsorbed water. The band at 2924 cm^{-1} can be attributed to C-H stretch, possibly from the CH_3/CH_2 group, and the strong band observed between 1590 and 1640 cm^{-1} may be due to C=C stretching vibration of alkenes or aromatic compounds or from C=O carbonyl stretching. The medium band observed between 1390 and 1380 cm^{-1} is assigned to the C-H bending, and the one that appears in the region between 1230-1270 cm^{-1} and the band between 1030 to 1075 cm^{-1} arises from C-O stretching vibrations. The band observed at 671.11 cm^{-1} may originate from out-of-plane bending of the aromatic C-H bond. The aqueous extract of *Ocimum kilimandscharicum* is rich in carbohydrates, reducing sugars, proteins, tannins and phenolics.[14,15] The FTIR spectra suggest that these biomolecules act as capping or stabilising agents in NPs synthesis. The peak at 532 cm^{-1} can be assigned to Ag-Cl stretching, and the narrow, sharp band at 2353 cm^{-1} possibly originates from O=C=O stretching of CO_2 adsorbed on nanoparticles.

SEM–EDX

To confirm the doping of Fe in Fe-doped Ag/AgCl NPs and that of Cu in Cu doped Ag/AgCl NPs, the samples were analysed by EDX. In the case of Cu doped Ag/AgCl nanoparticle, strong signals were observed from the silver at 3 keV and from chlorine at 2.6 keV (Fig.-3).

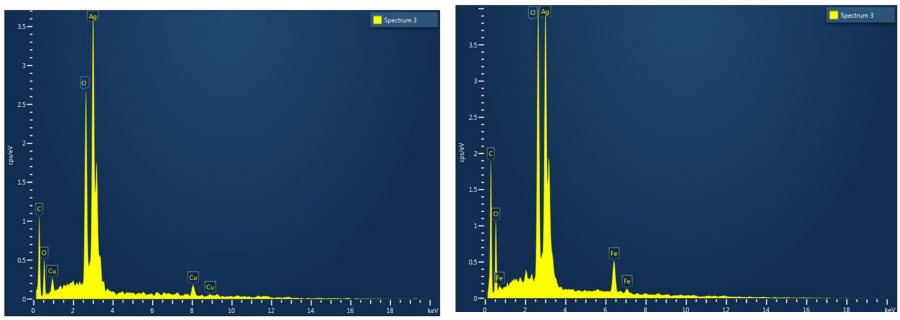

Fig.-3: EDX Spectra of the as-synthesised Cu and Fe Doped Ag/AgCl NPs

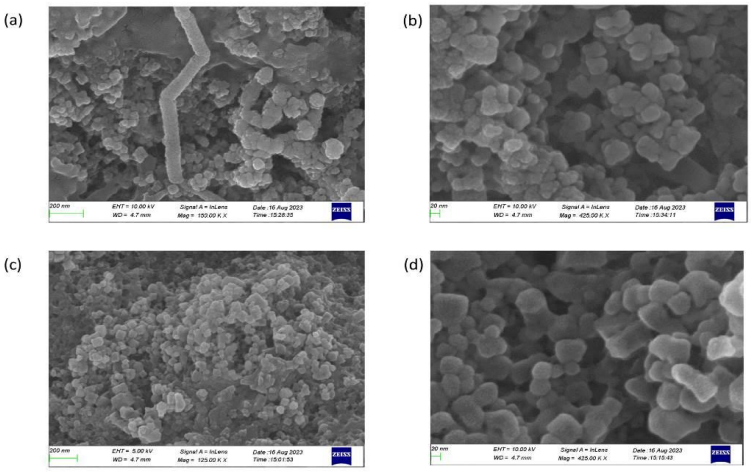

Fig.-4: SEM Image of the as-synthesized Cu Doped Ag/AgCl NPs (a and b) and Fe-doped AgCl NPs (c and d)

Signals for copper occur at 0.9 keV and 8 keV. This corroborates the findings of XRD and confirms the formation of Cu doped Ag/AgCl nanoparticles. In the case of Fe-doped Ag/AgCl nanoparticle, strong signals were observed from the silver at 3 keV and from chlorine at 2.6 keV. Signals for Iron occur at 0.7, 6.4 and 7KeV. This aligns with the findings of XRD and confirms the formation of Fe-doped AgCl nanoparticles. In both instances, signals for carbon occur at 0.3 KeV and for oxygen at 0.5 KeV. These data are in accordance with the suggestion that biomolecules from leaf extract act as a capping agent in NP synthesis. The SEM image of doped NPs reveal (Fig.-4) that Cu doped Ag/AgCl nanoparticles are irregularly shaped with rounded edges. The size of the nanoparticle varies between 10 and 50 nm, with an average size of 29 nm. In contrast, Fe-doped AgCl NPs were cube-shaped, and their size varied from 20 to 100 nm with an average of 46 nm.

Antibacterial Assay

The antibacterial effects of the samples were tested against 4 different species of bacteria by the Kirby-Bauer test (Fig.-5). Silver NP was found to be active against *Pseudomonas* at a 1mg/ml concentration. and against *Pseudomonas, Bacillus* and *Staphylococcus sp* at 10 mg/ml concentration (Table-2). Fe-doped Ag/AgCl NP was found to be effective against *Pseudomonas* and *Bacillus sp* at 10 mg/ml concentration. Cu doped Ag/AgCl NP was also found to be effective against *Pseudomonas, Bacillus* and *Staphylococcus sp* at a 10 mg/ml concentration. The zone of inhibition of Cu doped Ag/AgCl NP was found to be greater than that of Ag Np at this concentration indicating that it is more effective than the latter. This improved effectiveness was also observed at lower concentrations. (1mg/ml conc) against *Pseudomonas, Bacillus*

and *Staphylococcus sp*. In the case of *Pseudomonas*, a greater zone of inhibition was observed in Cu doped Ag/AgCl NP than in Ag. At this concentration, Ag NP was ineffective against *Bacillus* and *Staphylococcus,* while a zone of inhibition was observed with Cu doped Ag/AgCl NP. No Zone of inhibition was observed in the *Escherichia coli* plates after incubation with any of the synthesised nanoparticles. Thus, we can conclude that among the synthesised nanoparticles, Cu doped Ag/AgCl NP was the most effective against *Pseudomonas*, *Bacillus* and *Staphylococcus sp*.

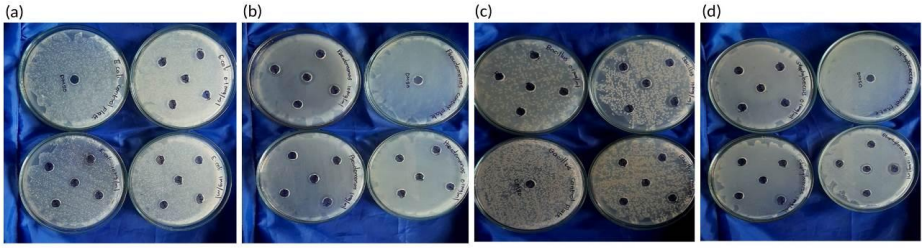

Fig.-5 Antibacterial Activity of Synthesised Ag/AgCl, Cu, Fe, Cu Doped Ag/AgCl and Fe-doped Ag/AgCl NP against (a) *Escherichia coli* (b) *Pseudomonas Sp* (c) *Bacillus Sp* (d) *Staphylococcus Sp*

Table-2: Antibacterial Activity of Synthesised Nanoparticle Ag, Cu-doped Ag/AgCl and Fe-doped Ag/AgCl against Gram Positive and Gram-Negative Bacteria

Bacterial culture	Control (DMSO)	Conc. of the Sample	Ag/AgCl	Fe	Cu	Cu doped Ag/AgCl	Fe-doped Ag/AgCl
Escherichia coli	-	0.1 mg/ml	-	-	-	-	-
		1mg/ml	-	-	-	-	-
		10 mg/ml	-	-	-	-	-
Pseudomonas Sp	-	0.1 mg/ml	-	-	-	-	-
		1mg/ml	13mm	-	-	15mm	-
		10 mg/ml	15mm	-	-	16mm	15mm
Bacillus Sp	-	0.1 mg/ml	-	-	-	-	-
		1mg/ml	-	-	-	11mm	-
		10 mg/ml	13mm	-	-	14mm	12mm
Staphylococcus Sp	-	0.1 mg/ml	-	-	-	-	-
		1mg/ml	-	-	-	13mm	-
		10 mg/ml	13mm	-	-	15mm	-

CONCLUSION

The study successfully demonstrated one-pot green synthesis of Fe and Cu doped Ag/AgCl nanoparticles using *Ocimum kilimandscharicum* leaf extract, an innovative and environmentally friendly method of synthesis that bypasses the use of harsh chemicals and aligns with Sustainable Development Goal 12 - responsible consumption and production. Addition of *Ocimum kilimandscharicum* leaf extract to silver nitrate led to the formation of Ag/AgCl NPs. On doping with copper, irregularly shaped Ag/AgCl NPs with rounded edges were formed. In contrast, doping with Fe resulted in the formation of cube-shaped AgCl NPs. XRD data also corroborates these findings. The presence of Cu in Cu doped Ag/AgCl and that of Fe in Fe-doped AgCl NPs were confirmed by EDX spectra. Ag/AgCl NPs, Cu doped Ag/AgCl NP and Fe-doped AgCl NPs were all effective against bacterial strains of *Pseudomonas, Bacillus* and *Staphylococcus Sp.* Among the doped NPs, Cu doped Ag/AgCl NP was more effective against bacteria than Fe-doped AgCl NPs. Thus, this study highlights how doping can play a significant role in enhancing antibacterial efficacy and in modulating the morphological characteristics of nanoparticles.

CONFLICT OF INTERESTS

The authors declare that there is no conflict of interest.

AUTHOR CONTRIBUTIONS

The present work is related to *SDG-12: Responsible Consumption and Production.* All the authors contributed significantly to this manuscript, participated in reviewing/editing and approved the final draft for publication. The research profile of the authors can be verified from their ORCID ids, given below:

T. Geetha https://orcid.org/0000-0002-4926-2701
John K Smitha https://orcid.org/0000-0001-8265-6297
Litty Mathew Irimpan https://orcid.org/0000-0002-5877-4573
Manju Sebastian https://orcid.org/0000-0003-3903-7911
C. J. Theresa https://orcid.org/0009-0009-6755-7907
Bincy Joseph http://orcid.org/0009-0004-7173-2337
M. Nancy http://orcid.org/0000-0001-5766-0331
K. Nimmy https://orcid.org/0000-0002-6665-0343
K. C. Dhanya http://orcid.org/0000-0001-9856-2842

Cite this article as: T. Geetha *et al.*, *Rasayan J. Chem.*, 19(2), 914-920(2026), https://doi.org/10.31788/RJC.2026.1929607.

REFERENCES

1. P. Thirubuvanesvari-Duraivelu, Siti Salwa Abd Gani, Masriana Hassan, Mohd Izuan Effendi Halmi, Reem Fawaz Abutayeh, Mohammad A. A., AlNajjar and Ala Abu-Odehe. *RSC Advances*, **15(34)**, 27723 (2025), https://doi.org/10.1039/D5RA03020J
2. A. Sati, T. N. Ranade, S. N. Mali, H. K. Ahmad Yasin and A. Pratap, *ACS Omega*, **10(8)**, 7549 (2025), https://doi.org/10.1021/acsomega.4c11045
3. X. Fan, L. Yahia, and E. Sacher, *Biology*, **10(2)**, 137(2021), https://doi.org/10.3390/biology10020137
4. Larranaga-Tapia M, Betancourt Tovar B, Videa M, Antunes Ricardo M, and Cholula Díaz J L, *Nanoscale Advances*, **6(1)**, 51 (2024), https://doi.org/10.1039/D3NA00761H
5. M. R. S. Zaidan, A. Noor Rain, A. R. Badrul, A. Adlin, A. Norazah, and I. Zakiah, *Tropical Biomedicine*, **22(2)**, 165 (2005)
6. H. Veisi, B. Karmakar, T. Tamoradi, S. Hemmati, M. Hekmati, and M. Hamelian, *Scientific Reports*, **11(1)**, 1983 (2021), https://doi.org/10.1038/s41598-021-81320-6
7. R. Rawat, V. Tiwari, R. Singh, and I. S. Bisht, *Journal of Essential Oil Bearing Plants*, **20(5)**, 1331 (2017), https://doi.org/10.1080/0972060X.2017.1383190
8. O. A. Lawal, I. A. Ogunwande, O. E. Omikorede, M. S. Owolabi, F. F. Olorunsola, A. A. Sanni, K. O. Amisu and A. R. Opoku, *American Journal of Essential Oils and Natural Products*, **2(1)**, 41 (2014)
9. V. Gopinath, S. Priyadarshini, N. Meera Priyadharsshini, K. Pandian, and P. Velusamy, *Materials Letters*, **91**, 224 (2013), https://doi.org/10.1016/j.matlet.2012.09.102
10. S. Kota, P. Dumpala, R. K. Anantha, M. K. Verma, and S. Kandepu, *Scientific Reports*, **7(1)**, 11566 (2017), https://doi.org/10.1038/s41598-017-11853-2
11. C. Chankaew, S. Somsri, W. Tapala, S. Mahatheeranont, C. Saenjum, and A. Rujiwatra, *Particuology*, **40**, 160 (2018), https://doi.org/10.1016/j.partic.2017.11.003
12. J. L Torres Lopez, S. Lazaro Mass, S. De la Rosa Garcia, *Journal of Cluster Science*, **36(1)**, 20 (2025), http://doi.org/10.1007/s10876-024-02722-w
13. Cameron F. Holder and Raymond E. Schaak, *ACS Nano*, **13(7)**, 7359 (2019), https://doi.org/10.1021/acsnano.9b05157
14. S. Selvarani and P. M. Vinayaga, M. Ramalakshmi, S. Padmapriya, M. Abirami, *Journal of Nanomaterials and Molecular Nanotechnology*, **5(2)**, 179(2016), https://doi.org/10.4172/2324-8777.1000179
15. M. S. Paschapur, M. B. Patil, R. Kumar and S. R. Patil, *International Journal of PharmTech Research*, **1(3)**, 544(2009)

[RJC-9607/2026]